ELECTROMAGNETIC SHIELDING EFFECTIVENESS OF HYBRID FIBRE REINFORCED COMPOSITES SUBJECTED TO LOW VELOCITY IMPACT

M. Siwak[1], E. Mikinka[2], I. Majsterek[1], K. Dragan[3] and P. Synaszko[3]

[1] Department of Clinical Chemistry and Biochemistry, Medical University of Lodz, Lodz, Poland, Mateusz.siwak@umed.lodz.pl, zchbk.umed.pl
[2] Department of Aeronautical and Automotive Engineering, Loughborough University, Loughborough, United Kingdom, e.e.mikinka@lboro.ac.uk, lboro.ac.uk/departments/aae/
[3] Division of Airworthiness, Air Force Institute of Technology, Warsaw, Poland, itwl.pl/en/

Keywords: hybrid composites, EMI shielding, impact damage

ABSTRACT

Despite increased interest in investigating electromagnetic shielding properties of carbon fibre reinforced composites, relatively little attention has been given to hybrid carbon/glass fibre composites and the topic of electromagnetic shielding durability was not explored at all. This study aims to systematically evaluate the effect of low velocity impact damage on the shielding effectiveness (SE) of both pure carbon and hybrid carbon/glass fibre reinforced composites in various lay-ups, with particular attention paid to establishing the threshold for SE reduction. All measurements were performed in the high frequency range of 26-42 GHz using free-space method with focusing lenses to concentrate the electromagnetic beam onto the damaged region of the sample. The responses for both damaged and undamaged specimens were compared to assess the effect of damage on the shielding properties. Splitting of carbon fibres on the non-impacted surface was found to remarkably reduce the SE of carbon/epoxy laminates, provided that the bottom ply was oriented parallel to the incident electric field direction. Hybridisation was most efficient when glass fibres were placed on both outer surfaces of the laminate as both impact surface fracture and carbon fibre splitting on the bottom surface were inhibited. In thin laminates the electromagnetic shielding durability was strongly affected by the lay-up, improving with the increasing number of carbon fibre plies oriented parallel to the electric field. The effect of repeated impact resembled that of increasing impact energy. Unidirectional hybrid lay-up provided better durability compared to the cross-ply one due to the smaller susceptibility to delamination damage accumulation. It has been demonstrated that due to the synergistic effects, properly designed hybrid carbon/glass fibre composites constitute an efficient material for lightweight damage tolerant shielding structure, whose electromagnetic shielding properties are maintained even after sustaining considerable mechanical damage.

1 INTRODUCTION

Electromagnetic interference (EMI) can deteriorate functioning of important electronic devices and in extreme cases lead to their complete breakdown. Shielding structures such as enclosures can serve as a barrier preventing penetration of unwanted electromagnetic (EM) radiation by reflecting and/or absorbing it. Due to very high electrical conductivity, metals offer excellent shielding capabilities but their disadvantages including high density, lack of design flexibility and susceptibility to corrosion have encouraged active search for alternatives. Continuous carbon fibre reinforced composites have emerged as an optimum balance between electrical and mechanical properties with additional advantages of chemical inertness and ability to tailor the design to the specific application. However, as opposed to the monolithic metallic structures which plastically deform under mechanical stimulus such as impact, CFRP composites absorb large amounts of energy in a number of failure mode such as matrix shear cracking, delamination and in extreme cases also fracture of the fibres. Their adverse effect on the CFRP mechanical properties, in particular compressive strength, is widely recognised and often results in a substantial overdesign of the composite components, counteracting their weight and cost-saving benefits. However, the possible detrimental effect of the impact-related damage has not been appreciated in the context of EM shielding properties with the only reported work on the EM shielding durability appearing against a backdrop of self-healing materials [1-2], where the emphasis was put on the ability to recover the shielding properties rather than understanding the effect the damage itself. The data for CFRP composites has been restricted to artificial delaminations and cut slits [3]. More efforts are therefore needed to obtain a deeper understanding of the EM shielding durability of fibre reinforced composites.

Hybridisation with glass fibre reinforced polymer (GFRP) plies is one of the strategies for improving the damage resistance of CFRP composites. Unlike carbon fibres, glass fibres are not electrically conductive, which means that they cannot be applied directly as shielding structures. Moreover, their general mechanical characteristics including strength and modulus is generally worse; they are also heavier compared to the carbon fibres. At the same time, however, glass fibres are more cost-effective and exhibit higher strain to failure, which is advantageous for impact damage absorption and containment. Consequently, laminates with hybrid glass and carbon fibre reinforcement constitute an optimum trade-off between cost, mechanical performance and damage resistance, but their EM shielding properties, with few exceptions [4-5], have not been investigated so far. The research presented in this paper extends the concept of damage tolerance to EM shielding properties by a systematic study on the EM shielding durability of hybrid carbon/glass fibre reinforced composites. In the presence of the impact damage of varying severity, the shielding effectiveness of the composite laminates is methodologically assessed with the aim of establishing the relationship between the degree of damage and possible impairment of the EM shielding properties. The study involving laminates with changeable location of glass fibre plies and various lay-ups such as unidirectional and cross-ply, placed at different angles relative to the electric field, enables identification of an optimum configuration for electromagnetically durable composites. In this way, a more cost-effective approach to the design of EM shielding composites can be developed.

2 FUNDAMENTALS OF EMI SHIELDING THEORY

Penetration of the EM field through a material barrier can be performed by implementing the transmission line (TL) formalism, where the panel is conceptualised as a two-port network [6]. Under the assumption that the planar material is illuminated with a normally incident EM plane wave, the tangential electric (E) and magnetic (H) field components at the front and back shield faces can be computed by solving Maxwell propagation equations:

$$dE/dx=-j\omega\mu H, \tag{1}$$

$$dH/dx=-j\omega\varepsilon E. \tag{2}$$

where ω is the angular frequency of the incident radiation; μ and ε correspond to the magnetic permeability and electric permittivity of the shielding screen material. The boundary conditions are applied based on the assumption that the panel is surrounded by air. The fields on the incident side (E_{in}, H_{in}) and transmission side (E_{out}, H_{out}) are related by the transmission matrix Φ:

$$\begin{bmatrix} E_{out} \\ H_{out} \end{bmatrix} = [\Phi] \begin{bmatrix} E_{out} \\ H_{out} \end{bmatrix}, \tag{3}$$

$$[\Phi] = \begin{bmatrix} \Phi_{11} & \Phi_{12} \\ \Phi_{21} & \Phi_{22} \end{bmatrix} = \begin{bmatrix} \cosh(\gamma d) & -\eta * sin\mathrm{h}(\gamma d) \\ -\frac{1}{\eta} * sin\mathrm{h}(\gamma d) & \cosh(\gamma d) \end{bmatrix}, \tag{4}$$

in which γ is the complex propagation coefficient, η is the intrinsic impedance and d is the thickness of the shield. If the material is highly conductive so that its permittivity is dominated by the conductivity σ, these complex electromagnetic properties reduce to:

$$\gamma = \frac{1+j}{\delta} \tag{5}$$

$$\eta = \sqrt{\frac{j\omega\mu}{\sigma}} \tag{6}$$

The skin depth δ is calculated from:

$$\delta = \frac{1}{\sqrt{\pi f \mu \sigma}} \tag{7}$$

where f is the frequency of the EM wave. Assuming that the panel is situated in the free space with impedance η_o, the transmission coefficient T can be derived as:

$$T = \frac{2\eta_o}{\Phi_{11}\eta_o - \Phi_{12} - \Phi_{21}\eta_o{}^2 + \Phi_{22}\eta_o} \tag{8}$$

which is directly used to obtain the total SE:

$$SE = 20 * log\left(\frac{1}{|T|}\right) \tag{9}$$

3 MANUFACTURING OF COMPOSITE MATERIALS

The manufacturing process of both baseline carbon fibre and hybrid carbon/glass fibre reinforced composites was realized in the autoclave. A unidirectional carbon fibre and 2/2 twill glass fibre reinforced prepregs supplied by Easy Composites (both under XC130 designation) were cut and laid-up in various arrangements which are summarized in Table 1. The stacks were cured according to the manufacturer's recommendations for 8 hours at 90ºC under the pressure of 0.62 MPa. The cured laminates were cut into square 150x150 mm samples for further testing using water-cooled bench saw with a diamond-coated cutting disk.

Test group	Sample Designation	Lay-up	Impact test energies
Carbon/epoxy	*CCCC-4AP*	[$C_{-45}/C_{45}/C_{45}/C_{-45}$]	5-9J
	CCCC-4CP	[$C_0/C_{90}/C_{90}/C_0$]	
	CCCC-4QI	[$C_{45}/C_0/C_{-45}/C_{90}$]	
	CCCC-4UD	[$C_0/C_0/C_0/C_0$]	3-7J
Thick hybrid	*CCCCG-4AP*	[$C_{-45}/C_{45}/C_{45}/C_{-45}/G_w$]	9-15J
	GCCCC-4AP	[$G_w/C_{-45}/C_{45}/C_{45}/C_{-45}$]	
	GCCCCG-4AP	[$G_w/C_{-45}/C_{45}/C_{45}/C_{-45}/G_w$]	
Thin hybrid	*GCCG-2AP*	[$G_w/C_{45}/C_{-45}/G_w$]	3-7J
	GCCG-2CP	[$G_w/C_0/C_{90}/G_w$]	
	GCCG-2UD	[$G_w/C_0/C_0/G_w$]	

Table 1: Composite configurations investigated in the study.

4 EXPERIMENTAL METHODS

4.1 Introduction of low-velocity impact damage to the composites

Controlled impact damage was introduced to the composite specimens using Instron Dynatup 9250HV Impact Testing machine. The impactor weighting 5.97 kg had a hemispherical nose with a diameter of 20 mm. A digital data acquisition module within the impactor was used to record the force-time response for each impact. The impact energies dependent on the lay-up were varied by adjusting the drop height. The range of energies for each laminate group is shown in Table 1. They were chosen to induce a visible damage in the laminates, including fibre fracture, but without penetrating the specimen, except for two cases of repeated impacts. The tested specimen was placed onto the frame fixture and clamped using a steel plate with central 80mm diameter hole to prevent out of plane motion of the sample and induce a possibly stiff response. To prevent multiple rebound impacts, a rebound catching mechanism was implemented.

4.2 Measurement of shielding effectiveness

For all SE measurements, modified free-space transmission technique was used, where the tested sample is place halfway between the transmitting and receiving antenna. The set-up, which is envisaged in Fig. 1a, consisted of two Flann22240 horn antennas connected to the ports of Anritsu MS46522B vector network analyser (VNA) with the help of lossless microwave coaxial cables. The experiments were conducted in the frequency range from 26 to 40 GHz. High impact polystyrene (ε_r=2.45) 3D printed focusing lenses with the diameter of 100mm and focal length of 131.6mm were placed in front of both antennas with a view to concentrating the radiated EM waves onto the damaged region of the specimen and avoiding diffraction effects at the sample edges while keeping the specimen dimensions to the minimum. During the experiment each sample was mounted over the 130 mm square aperture cut in the copper plate to reflect any waves that might otherwise be diffracted at the edges and maintain identical position of the specimen for each test. The large size of the copper plate (340x340 mm) was chosen to allow the slant path to be long enough for the sidelobe leakage to be outside the time domain window and time domain gating was implemented to separate specimen-related and other reflections within the set-up. The tested specimen was pressed against the copper plate to provide a possibly good electrical contact. In the case of some hybrid samples, glass fibre layer on the contact surface may act like a gap inducing unwanted EM energy leakage due to the breach of electrical conductivity. To address this issue, the edges of these samples were machined using Dremel tool and copper shielding tape was applied over the entire perimeter. The SE was obtained from the difference in the measured transmission parameter S_{21} for the cases with and without the sample in place according to equation:

$$SE=20*log|S_{21\_no\_sample}|-20*log|S_{21\_sample}|, \tag{10}$$

Taking the advantage of the fact that the far-field main lobe of the pyramidal horn antenna can be approximated as a Gaussian source, the Gaussian quasi-optical beam theory was used to analytically study the radiation pattern and obtain main parameters of the beam. In particular, the modification of the beam by the focusing lenses can be described with the Gaussian approximation [7-8], which allows to choose appropriate dimensions in the set-up. If the distance between the antenna and lens is equal to the focal length, the output beam waist is constant, and the output waist radius is expressed as:

$$w_{o\ out}=f*\lambda_o/\pi/w_{o\ in}, \tag{11}$$

where f is the focal length, λ_o is the free-space wavelength of the incident radiation and $w_{o\ in}$ is the input beam waist radius obtained from the horn antenna maximum size a:

$$w_{o\ in}=0.32a, \tag{12}$$

Further analysis of the Gaussian quasi-optical beam theory indicates that at the focal plane the phase taper is minimized with infinite radius of curvature so that the resultant EM fields can be approximated as a plane-wave. All tested specimens were placed at the focal plane, so that the plane wave SE was measured. A diagrammatic representation of the Gaussian beam approximation is depicted in Fig. 1b.

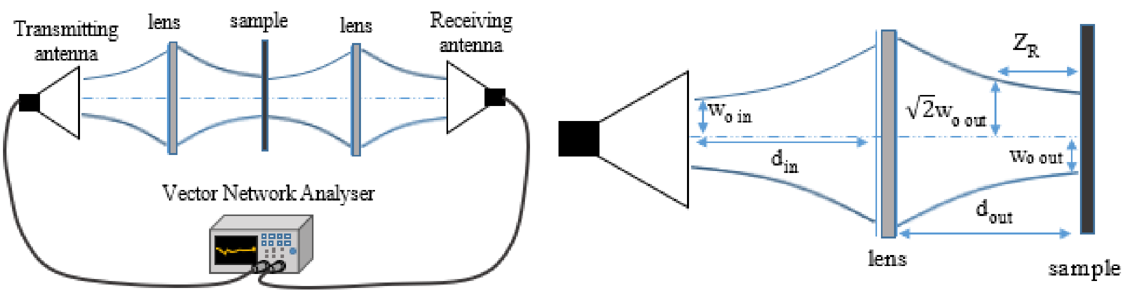

Figure 1: Shielding effectiveness measuring set-up.

5 RESULTS AND DISCUSSION

5.1 Impact damage characteristics

The recorded load-time response provided important information concerning damage mechanisms experienced by the laminates during the impact event. Shown in Fig. 2 are exemplary force-time curves, with the corresponding failure modes indicated. For the impacts with the lowest energy of 3J, a sinusoidal response was consistently observed; for these samples the damage state was limited to delamination, which was demonstrated by small changes of the slope in the loading part of the impact curve. With the increasing energy level, the force response curve was characterised by the truncated peak with multiple oscillations, indicating progression of fibre fracture and followed by slower recovery due to the resulting stiffness decrease. Moreover, in two cases of carbon fibre composites (cross-ply and quasi-isotropic) subjected to 9J impact, a sharp load drop was observed in the unloading part of the curve. After panel inspection this was attributed to the excessive push-out delamination of the rearmost layer as a result of large flexural stresses. The damage in these samples was marked by the carbon fibres being stripped off on the back surface and fractured on the top surface, although the impactor did not penetrate the specimen. The overall characteristics of the impact response for hybrid laminates was not significantly different in any aspect from that of pure carbon fibre composites.

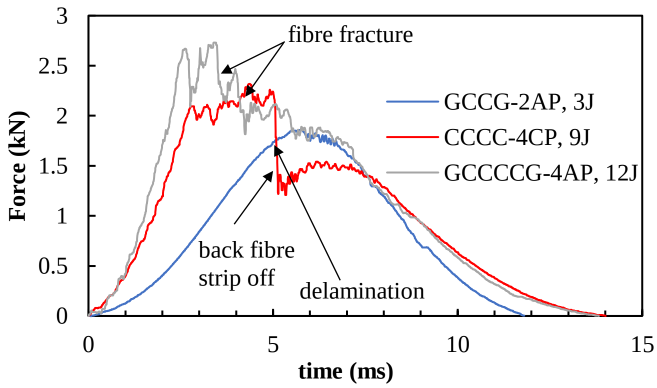

Figure 2: Examples of load-time responses for investigated composites.

Formation of the damage is closely associated with the amount of the impactor energy absorbed by the impacted specimen calculated from the area under load-displacement curve. The sub-perforation character of all impacts was confirmed by the ‘closed’ character of these curves. The fraction of the absorbed energy was increasing as the impact energy was rising. For the same impact energy, quasi-isotropic samples exhibited higher energy absorption than cross-ply and angle-ply although this did not translate into more severe damage state. In addition, all QI laminates were characterized by stiffest response which is believed to be associated with the higher number of dissimilar interfaces and shearing effect of the 0º/45º/90º interfaces. On the other hand, the damage initiation threshold and peak force remained approximately equal for all considered carbon/epoxy arrangements. This lack of trends can be ascribed to the heavy impactor/thin laminate combination, promoting dissipation of the energy in the form of fibre fracture instead of delamination creation, which is affected by the interfacial angle to the greatest degree.

Replacing outer carbon fibre plies with woven glass fibre layer was found to increase the impact energy absorption and alter the characteristics of the sustained damage while the response curves remained similar to those for pure carbon/epoxy composites. More specifically, all hybrid laminates demonstrated an enhanced ability to contain the damage to the vicinity of the contact zone of the impactor, preventing carbon fibre splitting or detachment on the back surface. With much higher strain-to-failure, glass fibres present on the outer surface were able to delay the breakage of the carbon fibres which were also shifted closer to the neutral plane in this configuration. In consequence, the bending stresses acting on them were reduced. Out of all configurations in the 'thick hybrid' group, the lowest damage resistance was observed in CCCCG configuration, whose absorbed energy fraction of 98.9% at 15J impact was at a transition between sub-perforation and perforation impact. Although the bottom glass fibres were able to prevent extensive carbon fibre splitting on the non-impacted side, the brittle carbon fibres on the impact surface were fractured, allowing for a deeper penetration of the impactor nose and severe reinforcement breakage in all subsequent plies. The opposite trend was observed when the glass fibre was moved to the impacted side. While the damage was more spread on the bottom surface with some of the carbon fibres pushed out, the continuity of the top face was maintained, which again was attributed to the better ability of glass fibres to accommodate deformation imposed by the hemispherical nose of the impactor. Finally, the most favourable impact resistance was achieved with glass fibres located on both outer surfaces of the laminate as not only the surface fracture was delayed but also the bottom carbon fibres did not split.

The character of the load response curve evolved when the specimen was impacted repeatedly at the same location, as shown in Fig. 3. Under the low energy level of 3J, the damage in the first impact was limited to delamination and matrix cracking exhibited as small changes in the slope of the rising portion of the load-time response curve having a primary Gaussian pulse shape. A slight increase in the slope was observed for the second impact, which can be attributed to the thin layer of unreinforced resin compacted during the first impact and providing harder surface for the next impact. The local fluctuations were also reduced in the loading part of the curve as the damage propagated along the direction of carbon fibres to the region already damaged by the first impact; the whole process was therefore more stable. A rapid load drop in the unloading part suggests onset of fibre fracture at the end of second impact and indicates a possible shift in the damage character from the matrix to fibre dominated, which was corroborated by the fibre fracture related peak force truncation and oscillations accompanied by a decrease in the laminate stiffness observed in subsequent third and fourth impact. The resulting increase in the impactor nose-composite contact area together with the reduced stiffness of the laminate were responsible for the prolonged impact duration. These observations held true for both angle-ply and unidirectional lay-ups, with the latter exhibiting better impact damage resistance and higher perforation threshold.

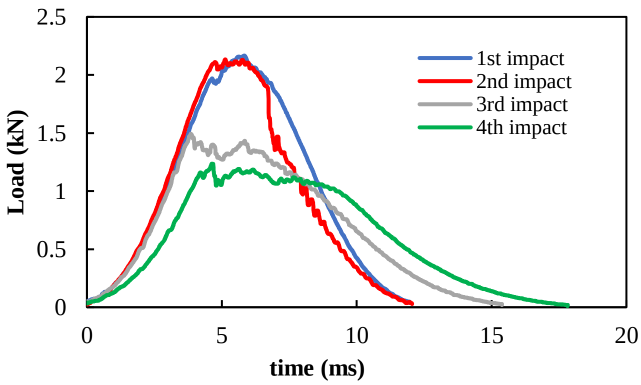

Figure 3: Load-time response curves for multiple 3J energy impacts on GCCG-2AP laminate.

5.2 Effect of impact damage on the shielding effectiveness of carbon/epoxy composites

In order to better understand the relation between the impact damage and SE of a composite, the measured SE was correlated with both the damage state of the composite (qualitative analysis) and impact conditions (quantitative analysis). Due to the different impact energy ranges, the three groups (carbon/epoxy, thick hybrid and thin hybrid) were considered separately.

After being impacted by low (5J) and medium (7J) energies, carbon/epoxy composites did not exhibit any noticeable change in the average SE. For these specimens, only indentation was observed on the impacted surface with some evidence of fibre splitting onset on the bottommost surface. The latter, however, did not impair the shielding capabilities of the laminate as the three preceding plies whose continuity was maintained, were able to provide attenuation within the dynamic range of equipment. For the largest impact energy of 9J, different trends were observed. Whereas no SE change was observed for 4-ply angle ply arrangement, both cross-ply and quasi-isotropic experienced a SE reduction not exceeding 10% (9.1% for the quasi-isotropic and 6.5% for the cross-ply). The damage state in these samples was characterised by the push-put delamination of the rearmost layer, accompanied by the fibre breakage on the impacted face. This combination allowed for a deeper penetration of the EM field and in consequence worse shielding properties. Slightly better performance of the cross-ply compared to the quasi-isotropic lay-up was ascribed to the larger amount of plies oriented parallel to the electric field, which ‘took over’ the attenuation functions of the most severely damaged plies. The average SE as a function of impact energy for the three carbon/epoxy composites is shown in Fig. 4.

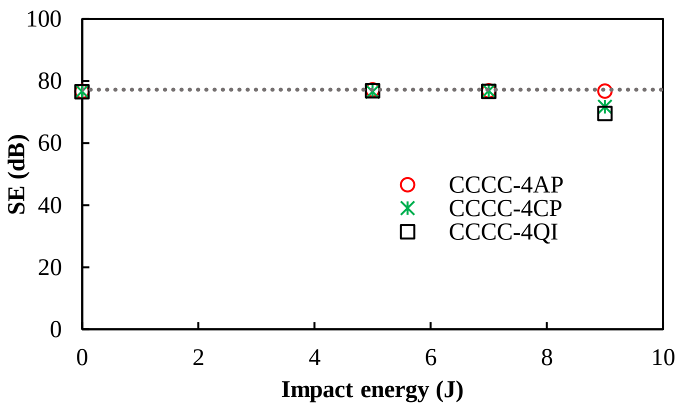

Figure 4: Average SE as a function of impact energy for carbon/epoxy composites. The dotted line indicates the average dynamic range of the set-up.

5.3 Effect of the glass fibre layer position on the electromagnetic shielding durability

The effect of the position of an additional glass fibre ply was investigated for the angle-ply lay-up, which demonstrated the most favourable electromagnetic shielding durability. In the three configurations considered, the glass fibre ply was placed on the top, bottom or both surfaces. The impact energy range was increased compared to the carbon/epoxy group to approach the damage resistance limits.

Placing glass fibre ply on the bottom surface limited the damage to the close vicinity of the impactor contact zone but did not prevent fibre fracture on the impacted surface due to the stresses exerted by the impactor when the impact energy was maximum. A very high fraction of the absorbed energy (98.9%) meant that the impactor was close to the perforating the specimen. The resulting reduction in the electromagnetic shielding reached 27% and was attributed to the interruption of the conductive carbon fibre network along the entire composite thickness. Moving the glass fibre ply to the top impacted surface resulted in a change in the observed damage characteristics. The carbon fibres on the non-impacted surface experienced extensive splitting with a small portion ripped off. However, the continuity of the impact surface was not compromised, which was attributed to a better ability of glass fibres to accommodate the deformation imposed by the hemispherical impactor. The fact that the structural integrity of the first ply was preserved, reduced the detrimental effect of broken carbon fibres in the bottommost ply which resulted in a smaller, 18.4% reduction in the average SE. This decrease was ascribed to the smaller effective shielding thickness in the vicinity of the impact zone, as the bottom surface carbon fibres were broken and detached. Finally, the presence of glass fibres on both outer surfaces gave the most favourable EM shielding durability as the SE was not reduced under the maximum energy impact. Although some fibre fracture could be inferred from the impact load responses, the glass fibre plies prevented both the impact surface fracture and back surface fibre splitting and detachment, keeping the laminate ‘compact’. As a result the continuity of the conductive network was maintained and the shielding capabilities were not compromised. SE as a function of frequencies for all three hybrid configurations after sustaining a 15J impact is shown in Fig. 5

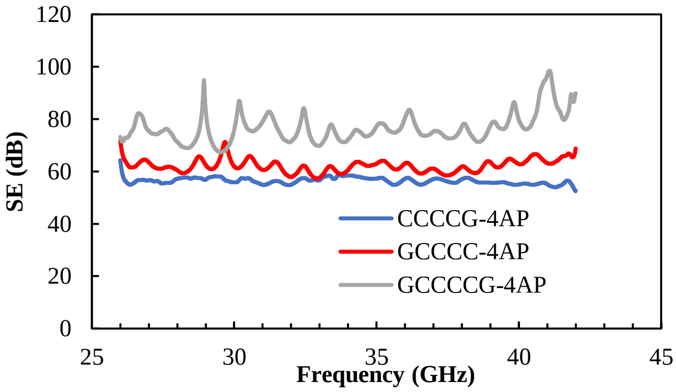

Figure 5: SE spectra for thick hybrid composites after 15J impact.

5.4 Electromagnetic shielding durability of thin hybrid laminates

Thinner laminates constitute a more cost-effective option when the material is not expected to be exposed to the most severe damage conditions. Given very high EM attenuative properties exhibited even by a single carbon fibre/epoxy ply, in the third ‘thin hybrid’ group, the number of carbon/epoxy plies was reduced by half. Based on the outcomes of the parametric study on the hybridisation architecture for thick hybrid composites, glass fibre plies were placed on both outer surfaces. Due to the reduced stiffness of the thin laminates, the incident impact energy was reduced to the maximum of 7J in order to avoid specimen penetration. A plot showing average SE as a function of impact energy for all three lay-ups is shown in Fig. 6.

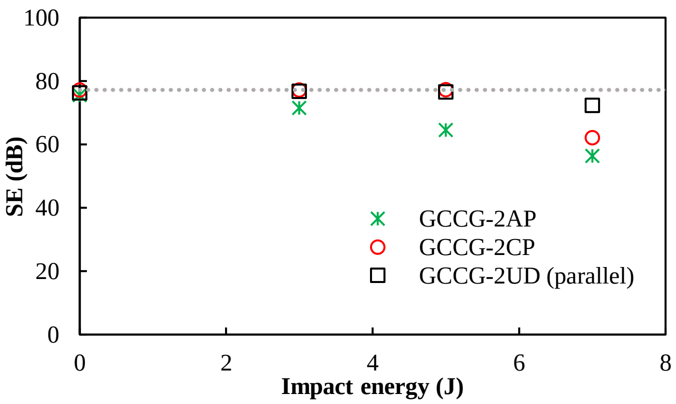

Figure 6: Average SE as a function of impact energy for thin hybrid composites.

A gradual reduction of SE with the impact energy was observed for the laminate with the angle-ply lay-up, reaching 25% decline for the most severe 7J impact. This trend is believed to be associated with the equal contributions of the two conductive carbon fibre plies to the total shielding, which is different from the other two lay-ups, where at least one parallel-oriented ply provided maximum shielding capabilities. In consequence, a slightly better EM shielding durability is obtained for the cross-ply lay-up, whose maximum reduction in the average SE for the highest energy impact did not exceed 20%. In both cases this decrease is associated with the partial breakage of the carbon fibres under the forces exerted by the heavy impactor which was confirmed both by the visual inspection of the impacted specimens and load-time curves.

For thin hybrid unidirectional composites, the electromagnetic shielding durability was determined by the angle at which the sample was oriented with respect to the electric field radiated from the horn antenna. When positioned in the parallel orientation, the SE of GCCG-2UD was not compromised until sustaining 7J impact damage, when a 5% reduction was noticed. This relatively small, compared to the other two lay-ups, decrease can be linked to the larger number of plies oriented to achieve the maximum possible shielding capability, so that even if some of the fibres experienced significant breakage, the remaining part could overtake the shielding functions, diminishing the harmful effect of the structural damage.

In the case of mutually perpendicular carbon fibres and electric field lines, the effective electrical conductivity was substantially reduced, increasing the EM penetration depth. This translated into a more significant role of the absorption loss. Electromagnetic shielding durability showed an increasing trend for the low and medium energy impacts (9.5% and 11% increase respectively) but dropped by almost 4% for the highest energy impact. The initial enhancement was most likely associated with the interlaminar damage in the form of delamination between the glass and carbon fibre plies. With the delamination created, not only was the effective thickness slightly increased but also the glass/carbon interfaces were split into a double-layer version with a thin air zone between them. As all three media exhibit different impedances, additional reflection coefficient term was present, which translated into a higher SE. When the impact energy increased, the character of the damage changed, with a more meaningful role of fibre damage. This meant coexistence of two competing mechanisms from the point of view of electromagnetic shielding capabilities and in consequence a small deterioration in SE. The average SE values of unidirectional samples after accommodating different levels of impact damage are summarized in Table 2 for both parallel and perpendicular laminate orientation.

Impact energy (J)	SE for parallel orientation (dB)	SE for perpendicular orientation (dB)
0	76.3	13.7
3	76.8	15.0
5	76.6	15.2
7	72.3	13.2

Table 2: Average SE of GCCG-2UD laminates after impact damage with varying energies in both parallel and perpendicular orientation.

5.5 Effect of multiple impacts on shielding effectiveness of hybrid laminates

Evolution towards more fibre dominated composite damage observed with the increasing number of equienergetic repeated impacts resulted in a gradual decrease in the shielding capabilities of angle-ply laminate reaching minimum of 40 dB for the penetrated composite as shown in Fig. 7. The trend, similar to that observed for the increasing impact energy level, see Fig. 6, is believed to be associated with the specific unfavourable arrangement of carbon fibres. Due to the large bending stiffness mismatch, the delamination damage appeared very early in the damage process and promoted quick evolution into more severe fibre fracture. Given that both carbon fibre plies were oriented at the same angle with respect to the electric field and therefore contributed equally to the shielding capabilities of the laminate, the reduction in SE originating from the interrupted electrical conductivity appearing with the fibre fracture was more pronounced than in the unidirectional lay-up having 90^{o} plies with the maximum shielding capabilities or less prone to early occurrence of delamination damage. For GCCG-2UD composite, different observations were made depending on how the laminate was oriented with respect to the electric field. The delamination created at the glass/carbon interface constituted additional internal reflection terms, which translated into a slightly improved SE for the laminate oriented perpendicularly to the electric field; the effect intensified originally with the increasing number of impacts but reversed as fibre fracture started to play a more significant role, which was the case for quadruple impact and perforated specimen. When the specimen was rotated by 90^o, the shielding durability was maintained until the perforation point, where a slight decrease appeared as a result of the interruption of the conductive network whereas the effect of delamination observed in perpendicular orientation was not detected due to the small skin depth of carbon fibres in the longitudinal direction and limited dynamic range of the measuring equipment. Anisotropic shielding characteristics of unidirectional composite under repeated impacts are shown in Fig. 8.

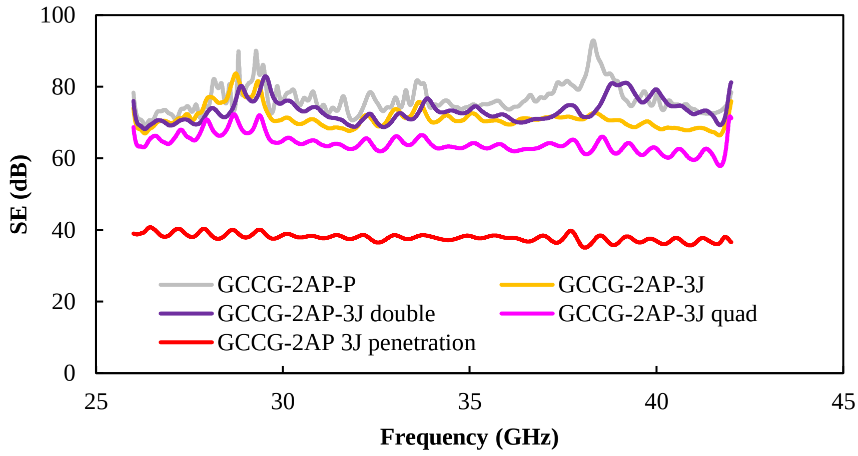

Figure 7: Evolution of SE with increasing number of impacts for GCCG-2AP composite.

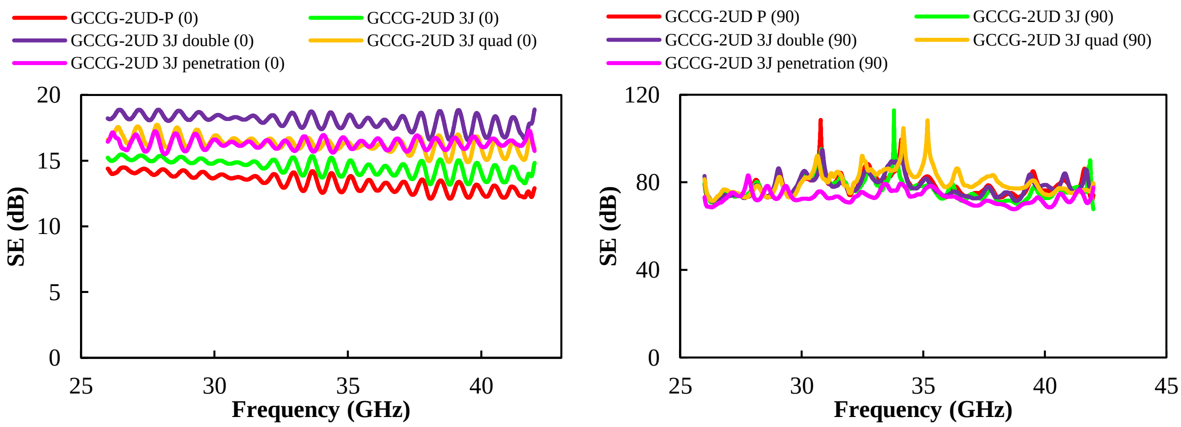

Figure 8: Evolution of SE with increasing number of impacts for GCCG-2UD composite in perpendicular (left) and parallel (right) orientation.

6 SUMMARY AND CONCLUSIONS

A correlation between the low velocity impact damage state and electromagnetic shielding properties was systematically examined for glass/carbon fibre reinforced hybrid composites in various lay-ups over a range of impact energies. The SE was measured before and after the impact event in 26-42 GHz frequency range using free-space technique with focusing lenses to concentrate the EM beam on the damaged region. A remarkable reduction in SE of carbon/epoxy was observed whenever the load exerted by the impactor caused excessive push out delamination of the rearmost layer, provided that it was oriented parallel to the incident electric field lines. This decline was ascribed to the combination of carbon fibre fracture compromising the electrical network continuity and reduction of the effective thickness weakening the absorption capabilities of the laminate. The effect of hybridization was strongly influenced by the position of glass fibre ply. Placement on the non-impacted surface, although limited the extent of back face carbon fibre splitting and detachment, did not prevent fracture of carbon fibres on the impact surface, allowing for the strongest EM energy penetration. With the glass fibres placed on the impacted side, the fracture of the conductive fibres was delayed thus improving the EM shielding durability. The arrangement with carbon fibre plies sandwiched between two glass fibre reinforced layers provided best damage resistance and electromagnetic shielding was not compromised even after sustaining impact of maximum energy. For thin laminates the EM shielding durability was found to be a strong function of the lay-up, and improved with the increasing number of carbon fibre plies oriented parallel to the electric field. The effect of repeated impact was similar to that of the increasing impact energy, with unidirectional arrangement exhibiting remarkably enhanced durability due to the smaller susceptibility to delamination damage accumulation. It was demonstrated that properly designed glass/carbon fibre laminates can be a cost-effective alternative for pure carbon/epoxy laminates in EM shielding applications.

ACKNOWLEDGEMENTS

The assistance of Max Farrand from Sports Technology Institute at Loughborough University in performing low-velocity impact tests is gratefully acknowledged.

REFERENCES

[1] T. Wang, W. Yu, C. Zhou, W. Sun, Y., Zhang, L. Jia, J. Gao, K. Dai, D. Yan and Z. Li, Self-healing and flexible carbon nanotube/polyurethane composite for efficient electromagnetic interference shielding, *Composites Part B*, **193**, 2020, pp. 108015 (doi: 10.1016/j.compositesb.2020.108015).

[2] H. Sim, D. Lee, H. Kim, Y. Jang, G. Spinks, S. Gambhir, D. Officer and S. Kim, Self-healing graphene oxide-based composite for electromagnetic interference shielding, *Carbon*, **68**, 2004, pp. 118-124 (doi: 10.1016/j.carbon.2019.08.073).

[3] Q. Ni, J. Hong, P. Xu, Z. Zu, K. Khovostunkov and H. Xia, Damage detection of CFRP composites by electromagnetic wave nondestructive testing (EMW-NDT), *Composites Science and Technology*, **210**, 2021, pp. 108839 (doi: 10.1016/j.compscitech.2021.108839).

[4] M. Gresil, and J. Janiszewski, High electromagnetic shielding effectiveness of hybrid glass/carbon composite laminate, *Proceedings of 9th International Symposium on Electromagnetic Compatibility joint with 20th International Wroclaw Symposium on Electromagnetic Compatibility, Wroclaw, Poland, September 13-17,* 2010, pp. 22.

[5] J. Gnidakouong, Y. Park, J. Keum, H. Jeong and Y. Jung, Multiscale hybrid composites for EMI shielding, *Proceedings of 18th International Conference on Composite Materials, Jeju, South Korea, August 21-26,* 2011, pp. 1-5.

[6] S. Schelkunoff, The electromagnetic theory of coaxial transmission lines and cylindrical shields, *Bell System Technical Journal,* **13**, 1934, pp. 532-579 (doi: 10.1002/j.1538-7305.1934.tb00679.x).

[7] P. Goldsmith, Quasi-optical techniques, *Proceedings of the IEEE,* **80**, 1992, pp. 1729-1747 (doi: 10.1109/5.175252).

[8] A. Kazemipour, The horn antenna as a Gaussian source in the mm-wave domain, *Journal of Infrared Millimeter and Terahertz Waves*, **35**, 2014, pp. 720-731 (doi: 10.1007/s10762-014-0077-9).